Received: 5 June 2018 | Accepted: 10 August 2018

DOI: 10.1002/jcp.27338

ORIGINAL RESEARCH ARTICLE

WILEY Journal of Cellular Physiology

Induction of apoptotic but not autophagic cell death by *Cinnamomum cassia* extracts on human oral cancer cells

Ching-Han Yu[1,2] | Shu-Chen Chu[3*] | Shun-Fa Yang[2,4] | Yih-Shou Hsieh[5,6] | Chih-Yi Lee[5] | Pei-Ni Chen[5,6]

[1]Department of Physiology, School of Medicine, Chung Shan Medical University, Taichung, Taiwan

[2]Department of Medical Research, Chung Shan Medical University Hospital, Taichung, Taiwan

[3]Institute and Department of Food Science, Central Taiwan University of Science and Technology, Taichung, Taiwan

[4]Medicine, Chung Shan Medical University, Taichung, China

[5]Institute of Biochemistry, Microbiology and Immunology, Chung Shang Medical University, Taichung, Taiwan

[6]Clinical Laboratory, Chung Shan Medical University Hospital, Taichung, Taiwan

Correspondence
Pei-Ni Chen, Ph.D., Institute of Biochemistry, Microbiology and Immunology, Chung Shan Medical University, No. 110, Section 1, Chien Kuo N. Road, Taichung 402, Taiwan.
Email: peini@csmu.edu.tw

Funding information
Ministry of Science and Technology Taiwan, Grant/Award Numbers: MOST 106-2320-B-040 -016, MOST 106-2320-B-040-020-MY3

Abstract

Cinnamomum cassia has been widely studied in different fields to reveal its antidiabetic, antidepressive, antiviral, anti-inflammatory, antiosteoporotic, and anticancer effects. Its antimalignant activities have been explored in lung cancer, breast cancer, colorectal cancer, and even oral cancer, but the detailed signaling mechanism and effects of this plant on animal models need to be clarified. In the current study, *C. cassia* extract (CCE) was used to investigate the antitumorigenesis mechanism in vitro and in vivo. The major constituents of CCE used in this study were coumarin, cinnamic acid, and cinnamic aldehyde. CCE reduced the viability, number, and colony formation of human oral cancer cells, and induced their apoptosis. Caspase-3 activation, Bcl-2 reduction, and phosphatidylserine inversion were involved in CCE-stimulated apoptosis. CCE also enhanced the expression of autophagic markers, including acidic vesicular organelle, microtubule-associated protein 1 light chain 3-I, autophagy-related protein 14, rubicon, and p62. The combined treatment of CCE and caspase inhibitor significantly restored mitochondrial membrane potential ($\Delta\psi_m$) and cell viability. However, the combined treatment of CCE and autophagy inhibitor further reduced the cell viability indicating that autophagy might be a survival pathway of CCE-treated SASVO3 cells. In contrast, CCE treatment for 12 days did not adversely affect SASVO3 tumor-bearing nude mice. CCE also elicited dose-dependent effects on the decrease in tumor volume, tumor weight, and Ki-67 expression. These results suggested that CCE showed the potential for the complementary treatment of oral caner.

KEYWORDS
apoptosis, autophagy, *Cinnamomum cassia*, oral cancer

1 | INTRODUCTION

Head and neck squamous cell carcinoma (HNSCC) include oral, oropharyngeal, and hypopharyngeal cancers. A total of 51,540 new cases of HNSCC and 10,030 deaths due to HNSCC are estimated in the United States in 2018 (Siegel, Miller, & Jemal, 2018). According to the statistical data from the Ministry of Health and Welfare, Taiwan, the mortality of HNSCC has increased from 7.1/100,000 persons to 10.4/100,000 persons in the past decade. With the increasing mortality of oral cancer, several approaches, such as surgery, chemotherapy, and radiotherapy, have been applied to treat patients. However, the 5-year recurrence and mortality rates of late-stage cancer (Stage III/IV) are still about 57% and 60%, respectively (Jacobson et al., 2012). Extracts from plant products, which are also

*Ching-Han Yu and Shu-Chen Chu contributed equally.

called nutraceuticals, have been considered as an alternative therapy for oral cancer. In our previous studies, these botanical compounds have physiological bioactivities targeting the multiple molecular pathways for cancer therapy (P. N. Chen et al., 2011; Hu et al., 2012). Therefore, the cancer chemopreventive effect of natural products needs to be evaluated.

The bark of *Cinnamomum cassia* has been obtained for use as a food spice and traditional medicine. The major constituents of *C. cassia* essential oil include cinnamic aldehyde, cinnamic alcohol, cinnamic acid, and coumarin (Liao et al., 2012). Recently, researchers have found that various bioactivities are evoked by *C. cassia* extract (CCE), such as prosexual effect (Goswami, Inamdar, Jamwal, & Dethe, 2014), anti-inflammation (Shin et al., 2017), antivirus (Fatima, Zaidi, Amraiz, & Afzal, 2016), antidiabetes (Ranasinghe et al., 2017; Song et al., 2017), antidepression (Zada et al., 2016), antiosteoporosis (Huh et al., 2015), and antitumorigenesis (Lin et al., 2017; Kianpour Rad et al., 2015). The mechanisms of cancer suppression induced by CCE include proapoptosis (Chang, Cheng, Wang, Chou, & Shih, 2017; Kianpour Rad et al., 2015), antimetastasis (Lin et al., 2017; H. C. Wu et al., 2018), and antiangiogenesis (E. C. Kim, Kim, & Kim, 2015). In other cases, the CCE treatment triggers and increases reactive oxygen species (ROS), resulting in mitochondrial membrane disruption and then caspase-mediated apoptosis (Kianpour Rad et al., 2015). In colon cancer, this CCE-induced ROS-dependent apoptosis is regulated by nuclear factor κB (NF-κB) and activating transcription factor 3 (ATF3; S. H. Park, Song, et al., 2018). The major compound of CCE, cinnamaldehyde, induces caspase-mediated apoptosis in non-small cell lung cancer by upregulating a novel circular RNA, hsa_circ_0043256 (Tian, Yu, Ye, & Wang, 2017). Proteases, such as matrix metalloproteinase and urokinase-type plasminogen activator, and Wnt/β-catenin pathway are downregulated by CCE treatment, thereby reducing cancer cell invasion (C. Wu et al., 2017; H. C. Wu et al., 2018). CCE also suppresses vascular endothelial growth factor (VEGF) expression and VEGF-mediated malignant outcomes, such as proliferation, migration, invasion, and metastasis of cancer cells (E. C. Kim et al., 2015). Thus, CCE shows strong potential to be used as a cancer therapeutic supplement; its detailed mechanisms and effects on the animals should be further explored.

In this study, 50% ethanol extract of *C. cassia* was obtained to treat human oral cancer in vitro and in vivo and determine the signaling pathway involved in CCE-induced anticancer effects.

2 | MATERIALS AND METHODS

2.1 | Cell culture

Four cell lines were received as gifts from Cheng-Chia Yu (Chung Shan Medical University, Taichung, Taiwan): OC2, which was derived from a Chinese man, is a cell line of oral buccal-mucosa squamous carcinoma, which can form tumors in nude mice (Wong, Chang, Chen, & Chang, 1990); SCC-4 is a human tongue squamous cell carcinoma (Bioresource Collection and Research Center, Hsinchu, Taiwan; P. N. Chen et al., 2006); SAS is a highly tumorigenic human tongue squamous carcinoma cell line (Japanese Collection of Research Bioresources, Tokyo, Japan; S. F. Chen et al., 2012); and SASVO3 is a highly malignant HNSCC cell line acquired from primary SAS tumors after three sequential rounds of xenotransplantation (C. Y. Chen et al., 2009). SAS and SASVO3 cells were cultured in Dulbecco's modified Eagle's medium (DMEM, Thermo Fisher Scientific Inc., Waltham, MA) containing 10% fetal bovine serum (FBS; Thermo Fisher Scientific Inc.) and 2 mM glutamine (MilliporeSigma, St. Louis, MO). SCC-4 cells were grown in DMEM–Ham's F-12 medium (Thermo Fisher Scientific Inc.) with 10% FBS, 2 mM glutamine, and 400 ng/ml hydrocortisone (MilliporeSigma). OC2 cells were cultured in Roswell Park Memorial Institute medium supplemented with 10% FBS. All of the cell lines were incubated in a humidified incubator with 5% CO_2 at 37°C.

2.2 | Preparation of CCE

C. cassia was purchased from a Chinese medicine store in Taichung, Taiwan. CCE was prepared as mentioned earlier (Lin et al., 2017). In brief, 100 g of air-dried branches were stewed with 500 ml of 50% ethanol at 70°C for 24 hr. The filtered broth was lyophilized and stored at −20°C. Furthermore, the chemical profile of CCE was examined using high-performance liquid chromatography (HPLC) mass spectrometer (Waters 600 with a 2998 Photodiode Array detector; Marshall Scientific, Hampton, NH). Samples (10 μl) were injected into a Merck LiChrospher 100 RP-18 column (4 mm × 250 mm; Merck KGaA, Darmstadt, Germany); and analyses were carried out using the mobile phase composed of two solvents: solvent A (0.05% acetic acid in water) and solvent B (acetonitrile). The flow rate was 1 ml/min. Elution was performed in a programmed gradient elution as follows: (a) elution with 0–60% B for the first 30 min; (b) isocratic elution with 100% B for 30–35 min; and (c) isocratic elution with 100% A for 35–40 min. Absorbance was determined at 280 nm.

2.3 | Cell viability and cell growth assay

The cells were seeded onto 24-well plates at a density of 4×10^4 cells/well for 24 hr and then treated with CCE for another 24 hr. Then, the cells were incubated with 0.5 mg/ml 3-(4,5-dimethylthiazol-2-y1)-2,5-diphenyltetrazolium bromide (MTT; MilliporeSigma) in a culture medium for 4 hr. Blue formazan crystals in viable cells were dissolved with isopropanol, and then OD value was evaluated at 563 nm (Lu et al., 2016). For cell growth assay, the treated cells were harvested and counted in duplicate by using a hemocytometer. Trypan blue exclusion assay was also performed to determine the viable and dead cells.

2.4 | Colony formation assay

Five thousand SASVO3 cells were plated as single cells in a six-well plate for 10 days. The cell culture medium was replaced with different concentrations of CCE (0, 25, 50, and 100 μg/ml) every 3 days. Colonies were stained with crystal violet (MilliporeSigma),

and the number of colonies was counted under a microscope. Three separate experiments were performed to determine the repeatability of the results.

2.5 | Cell cycle analysis

After cell seeding was conducted for 24 hr, SASVO3 and SAS cells were preincubated in a medium containing 8 mM glutamine and 0.04% FBS for another 24 hr (Ho et al., 2001). The cells were then treated with 0, 25, 50, and 10 μg/ml CCE in 10% FBS medium for 24 hr; collected, washed with phosphate-buffered saline (PBS); fixed in 70% ethanol at −20°C for 2 hr, and stained with propidium iodide (PI; MilliporeSigma) solution (25 μg/ml PI, 0.1 mM ethylenediamine-tetraacetic acid [EDTA; MilliporeSigma], and 10 μg/ml RNase in PBS) for 30 min in the dark. Chromosome proportion was determined using a FACScan laser flow cytometer (Becton Dickinson, San Jose, CA).

2.6 | Western blot analysis

The cells were treated with CCE for 24 hr and lysed using a cold mammalian protein extraction buffer kit (GE Healthcare Bio-Sciences Corp., Piscataway, NJ) with protease inhibitor cocktails for 20 min to prepare the total cell lysates. The samples were separated in a 12.5% polyacrylamide gel and then transferred onto a nitrocellulose membrane. Afterward, the membranes were blocked with 5% nonfat milk in Tris-buffered saline containing Tween-20 (20 mM Tris, 137 mM NaCl, pH 7.6, 0.1% Tween-20) for 1 hr and probed with antibodies specific for β-actin (sc-47778, 45 kDa; Santa Cruz Biotechnology Inc., Santa Cruz, CA), PI3K (P13020-050, 85 kDa; BD Transduction Laboratories, San Jose, CA), p-Akt (44-621G, 65 kDa; Invitrogen, Carlsbad, CA), activated caspase-3 (#9664, 19 kDa), Bcl-2 (#2876, 28 kDa), rubicon (#5465, 130 kDa), Becline-1 (#3495, 60 kDa), Atg7 (#2631, 78 kDa), Atg5 (#2630, 55 kDa), Atg14 (#5504, 65 kDa), LC3A (#4599, 14 and 16 kDa), p62 (#5114, 60 kDa), PI3K and mToR (#2983, 289 kDa; Cell Signaling Technology Inc., Danvers, MA) and corresponding peroxidase-conjugated anti-mouse IgG antibody (#7076) or anti-rabbit IgG antibody (#7074; Cell Signaling Technology Inc.). A signal was subsequently detected with enhanced chemiluminescence kit, and the relative density of specific protein was quantified with ImageQuant LAS 4000 Mini (GE Healthcare, Little Chalfont, UK; Huang et al., 2016). At the termination of the experiment in vivo, tumor samples were added with protein extraction buffer kit, homogenized at 4°C and kept on ice for 30 min followed by centrifugation at 10,000*g* for 30 min. Cell lysates were incubated with the activated caspase-3 antibody, washed, and monitored by immunoblotting using the anti-mouse secondary antibody.

2.7 | 4′,6-Diamidino-2-phenylindole (DAPI) staining

CCE-treated cells were washed twice with PBS, fixed in 70% ethanol at room temperature (RT) for 30 min, and stained with DAPI (0.6 μg/ml in PBS) for 5 min. Fluorescent-labeled chromatin was observed under an ultraviolet light microscope and apoptotic cells were morphologically defined on the basis of cellular shrinkage and chromatin condensation (P. N. Chen et al., 2005).

2.8 | Mitochondrial membrane potential ($\Delta\psi_m$) assay

CCE-treated cells were washed twice and incubated in a complete medium containing 10 μg of fluorescent lipophilic cationic JC-1 dye for 30 min at 37°C in the dark. The stained cells were collected, washed, resuspended, and subjected to immediate flow cytometry analysis. A selectively accumulated JC-1 dye was presented in intact mitochondria to form multimeric J-aggregates that exhibited an emission at 590 nm (red) with high membrane potential. A JC-1 monomer emitted fluorescence at 527 nm (green) with low membrane potential. Thus, the fluorescence color of JC-1 represented $\Delta\psi_m$, which can be analyzed using a fluorescence microscope (Mantena, Sharma, & Katiyar, 2006).

2.9 | Annexin V-FITC and PI staining assay

The CCE-induced apoptosis of SASVO3 cells was quantified through flow cytometry with annexin V binding and PI uptake. In brief, CCE-treated cells were collected, washed twice with PBS, and subjected to annexin V and PI by using Vybrant Apoptosis Assay Kit 2 (Thermo Fisher Scientific Inc.) in accordance with the manufacturer's protocol. After the cells were stained, flow cytometry was performed to quantify the apoptotic cells (Mantena et al., 2006).

2.10 | Detection of autophagic vacuoles

The monodansylcadaverine (MDC; MilliporeSigma) is an autofluorescent material recently discovered for autophagic vacuoles labeling. In this study, the CCE-treated cells were washed with Hank's balanced salt solution (HBSS; MilliporeSigma) twice, stained with 1 μg/ml MDC in HBSS containing 5% FBS for 15 min, washed with HBSS, covered with HBSS containing 5% FBS, and detected under a fluorescence microscope in green filter.

2.11 | Detection and quantification of the acidic vesicular organelle (AVO)

The occurrence of AVOs was assessed in accordance with a previously described procedure with certain modifications. The cells were treated with CCE for 24 hr, washed with HBSS twice after the treatment, stained with 1 μg/ml acridine orange (MilliporeSigma) in HBSS containing 5% FBS for 15 min, washed and covered with HBSS containing 5% FBS, and observed under a red-filtered fluorescence microscope (Hsin et al., 2011).

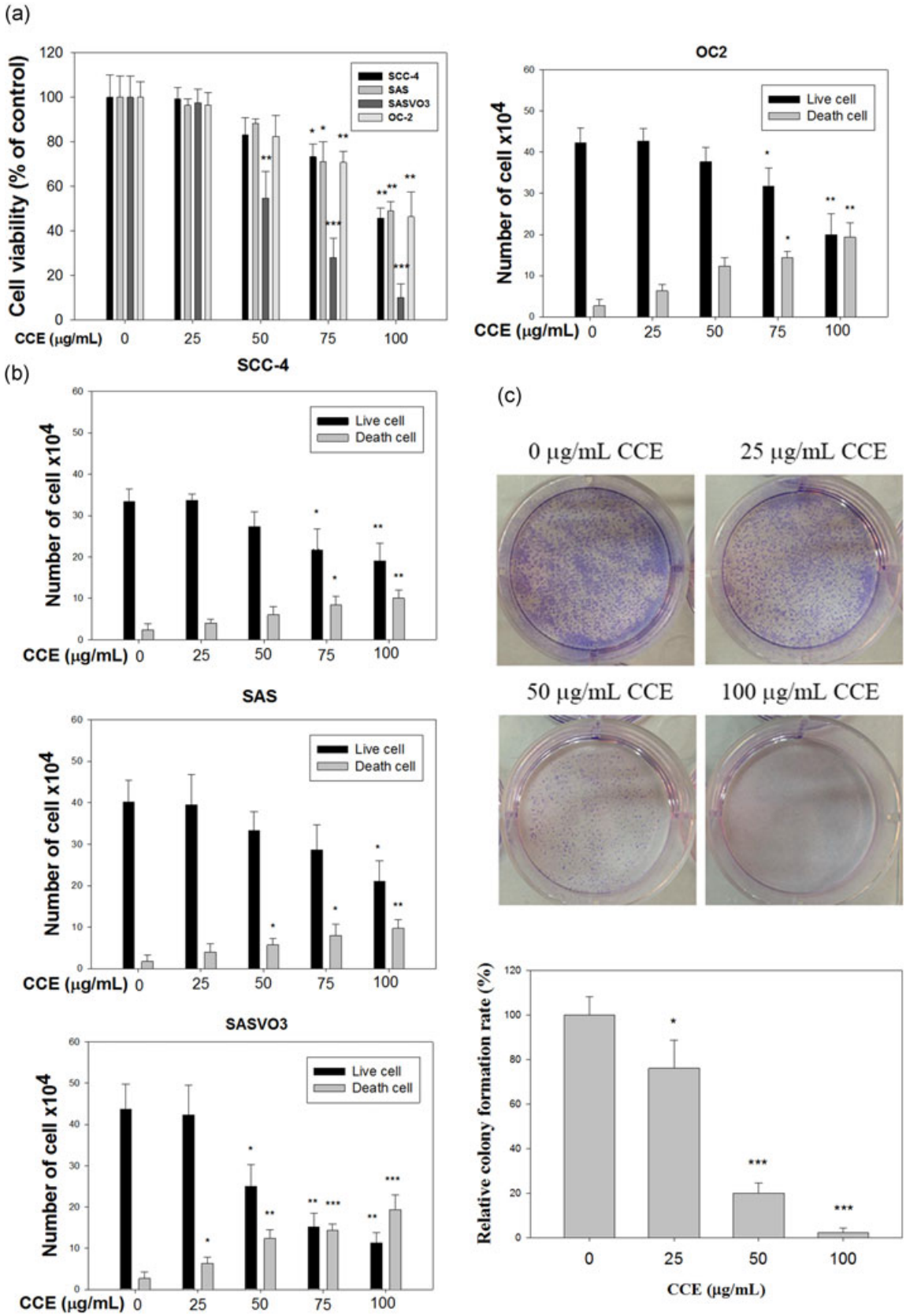

FIGURE 1 Effects of CCE on the viability and colony formation of oral cancer cells. (a) SCC-4, SAS, SASVO3, and OC2 cells were treated with various CCE concentrations for 24 hr. Cell viability was analyzed by MTT assay. (b) Cells were treated with CCE for 24 hr. Live and dead cells were then collected and counted using a hemocytometer. (c) Equal numbers of SASVO3 cells were plated and treated with various concentrations of CCE for 10 days. The number of formed cell colonies was counted. Data represented the mean ± *SD* of three independent experiments. $^{*}p < 0.05$, $^{**}p < 0.01$, and $^{***}p < 0.001$ compared with the control group. CCE: *Cinnamomum cassia* extract; MTT: 3-(4,5-dimethylthiazol-2-y1)-2,5-diphenyltetrazolium bromide; SCC: squamous cell carcinoma [Color figure can be viewed at wileyonlinelibrary.com]

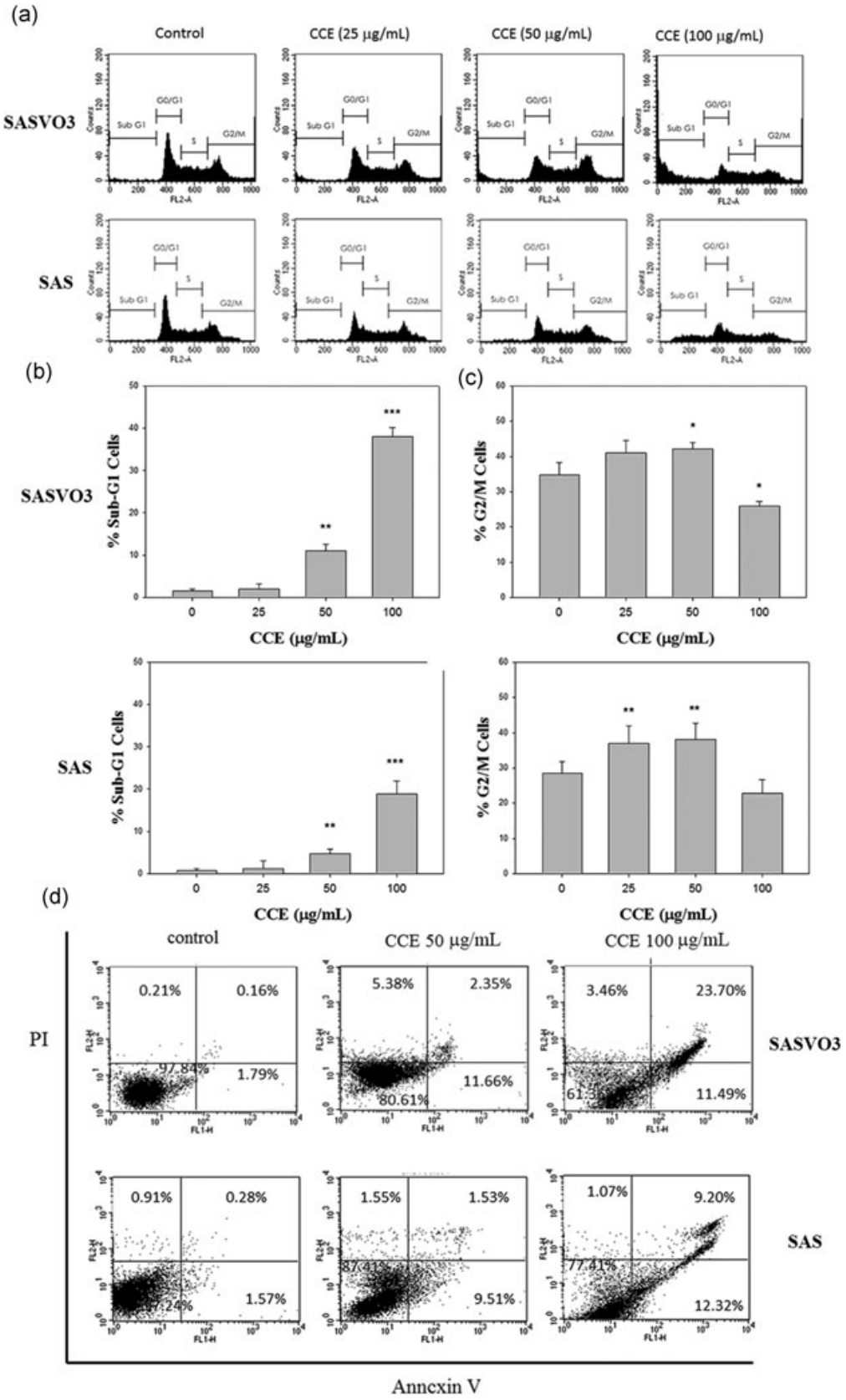

FIGURE 2 Induction of the apoptotic effect of CCE on oral cancer cells. (a) SASVO3 cells were treated with various CCE concentrations, and cell cycle distributions were assessed through flow cytometry with PI staining. Flow cytometry analysis with PI staining was conducted to determine the number of (b) sub-G1 cells and (c) G2/M cells. (d) Flow cytometry analysis with annexin V/PI double staining was carried out to examine the number of apoptotic cells. Data represented the mean ± *SD* of three independent experiments. $^{*}p < 0.05$, $^{**}p < 0.01$, and $^{***}p < 0.001$ compared with the control group. CCE: *Cinnamomum cassia* extract; PI: propidium iodide

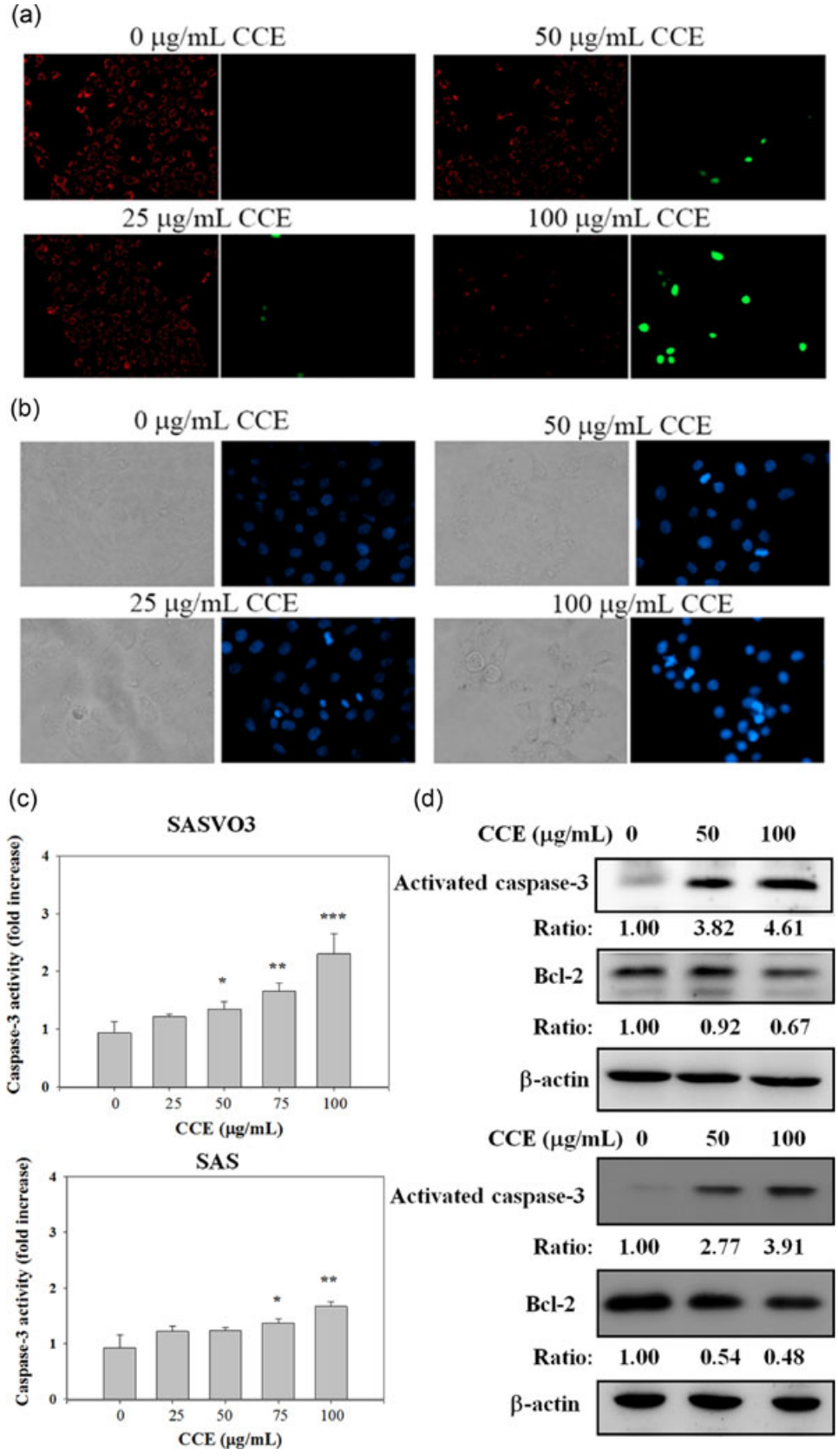

FIGURE 3 Continued.

2.12 | Caspase-3 activity assay

Caspase-3 activity was determined using the EnzChek® Caspase-3 Assay Kit #2 in accordance with the manufacturer's instructions (Thermo Fisher Scientific Inc.). In brief, the cells were harvested 24 hr after the treatment, washed in PBS, and lysed on ice for 30 min. Cell lysates were centrifuged and transferred to individual microplates, and background fluorescence was determined using a lysis buffer. An equal volume of 2× substrate working solution was added to each sample and control, and the plates were incubated in the dark at room temperature for 30 min. Fluorescence was determined using a Fluoromark plate reader (Bio-Rad, Hercules, CA) with excitation at 496 nm and emission at 520 nm. Fluorescence units were normalized against the total protein content.

2.13 | Detection of active caspase-3 and caspase-7

Intracellular caspase-3 and caspase-7 activities were quantified through fluorescence microscopy by using CellEvent™ Caspase-3/7 Green Detection Reagent (Thermo Fisher Scientific Inc.). The cells were seeded onto 96-well plates, pretreated with or without Z-VAD-Fmk for 2 hr, and then cultured with CCE for 24 hr. Afterward, 5 μM fluorescence reagent was added to the cells. The plates were incubated at 37°C with 5% CO_2 for 30 min and detected with a fluorescence microscope with the corresponding filter (green channel).

2.14 | Bioluminescence imaging (BLI) measurement of tumor growth in nude mice

Four- to five-week-old immunodeficient nude mice (BALB/c AnN. C*gFoxn*^{nu}/Crl Narl mice) were acquired to establish a mouse xenograft model and handled in accordance with the animal welfare regulations of the Institutional Animal Care and Use Committee (IACUC) of the Chung Shan Medical University (IACUC Approval Number: 1807). All of the mice were housed in a pathogen-free environment by using a 12-hr/12-hr light cycle at the Laboratory Animal Center. The mice could access standard rodent chow (Laboratory Rodent Diet 5001; LabDiet, St. Louis, MO) and water ad libitum. SASVO3 cells were transfected with the pGL4.50[luc2/CMV/Hygro] vector encoding the luciferase reporter gene luc2 (originating from the North American firefly, *Photinus pyralis*) was purchased from Promega Corporation (Madison, WI). Luciferase-transfected cells were cultured in the presence of hygromycin B (400 μg/ml; Life Technologies, Waltham, MA). Cells were subcutaneously injected into the right flank of the mice (5×10^6 cells/0.1 ml per mouse). On Day 10 postimplantation, the mice were randomly separated into three groups ($N = 5$ for each group). Sterile water (control) and CCE (250 and 500 mg·day^{-1}·kg^{-1}) containing sterile water were given to the mice via oral gavage. BLI was achieved using an IVIS50 animal imaging system (Xenogen Corp., Alameda, CA). Each mouse should receive 150 mg Luciferin/kg body weight. The luciferase activity in SASVO3 cells represented the tumor size. The photons emitted from the tumor penetrated the mammalian tissue and could be externally examined and quantified using a sensitive light imaging system (Hu et al., 2012).

2.15 | Immunohistochemistry analysis

Paraffin-embedded slides were deparaffinized, and the antigen was unmasked by microwave heating in citrate buffer for 20 min. The slides were then incubated with primary anti-Ki67 antibody and subsequently biotinylated secondary anti-mouse antibody (Hsieh et al., 2013). In immunohistochemistry, single immunohistochemical methods are used to detect one antibody-bound antigen using the chromogen 3,3′-diaminobenzidine, which is horseradish peroxidase (HRP) substrate that is used for secondary HRP-conjugated antibody detection.

2.16 | Statistical analysis

Results were analyzed through one-way analysis of variance with post hoc Dunnett's test and considered statistically significant at $p < 0.05$ (Sigma-Stat 2.0; Jandel Scientific, San Rafael, CA).

3 | RESULTS

3.1 | CCE-induced reduction of the viability of oral cancer cells

MTT assay revealed that CCE, especially at higher concentrations (75 and 100 μg/ml), significantly reduced the viability of various oral cancer cell lines after 24 hr of treatment. Among the four cell lines, CCE strongly inhibited the growth of SASVO3 cells (Figure 1a). Trypan blue exclusion assay demonstrated that the number of live cells decreased, whereas the number of dead cells increased in a dose-dependent manner after CCE treatments in SCC-4, SAS,

FIGURE 3 Apoptotic patterns of SASVO3 and SAS cells treated with CCE. Cells cultured with various CCE concentrations for 24 hr were examined for apoptosis. (a) Changes in $\Delta\Psi_m$ were assessed using a fluorescent lipophilic cationic JC-1 dye of the SASVO3 cells. JC-1 was selectively accumulated in intact mitochondria to form multimeric J-aggregates that emitted fluorescence at 590 nm (red) with a high membrane potential (left). Monomeric JC-1 emitted light at 527 nm (green) representing a low membrane potential (right). (b) Cells were stained with DAPI and detected under a UV light microscope to examine the nuclear morphology of the SASVO3 cells. Treatment of CCE showed the areas with intense fluorescence staining and condensed nuclei (at a magnification of ×200). (c) Caspase-3 activity was measured using an assay kit. (d) Western blot analysis was performed on activated caspase-3 (cleaved form) and Bcl-2 in both SAS and SASVO3 cells. β-Actin was used as a loading control. A result representing three separate experiments is shown. $^*p < 0.05$, $^{**}p < 0.01$, and $^{***}p < 0.001$ compared with the control group. CCE: *Cinnamomum cassia* extract; DAPI: 4′,6-diamidino-2-phenylindole; UV: ultraviolet [Color figure can be viewed at wileyonlinelibrary.com]

SASVO3, and OC2 cells (Figure 1b). Colony formation is an important aspect in tumor growth. As such, the number of colonies was counted after 10 days of treatment to determine the anticancer activity of CCE. The results indicated that the number of colonies decreased in a dose-dependent manner after CCE treatments in SASVO3 cells ($p < 0.001$; Figure 1c).

3.2 | CCE-induced apoptosis of SASVO3 and SAS cells

The cell cycle distribution of the CCE-treated SAS and SASVO3 cells were detected by PI staining. This assay revealed the cell apoptosis (sub-G1 elevation) and cell cycle arrest (G0/G1 accumulation or G2/M accumulation). A proportion of the cells in the sub-G1 phase significantly increased from 2% and 1% in the control group to 38% and 19% in the high-dose CCE group of SASVO3 and SAS cells, respectively (100 μg/ml, $p < 0.001$; Figure 2a,b). In Figure 2c, CCE increased the percentage of the G2/M population at 25 and 50 μg/ml in both SASVO3 and SAS cells. However, CCE significantly decreased the proportion of the G2/M population in the high-dose group of SASVO3 cells. Annexin V/PI staining indicated the apoptotic cell death (annexin V-positive cells in the lower right quadrant), necrotic cell death (PI-positive cells in the upper left quadrant), or combined cell death (annexin V/PI-positive cells in the upper right quadrant).

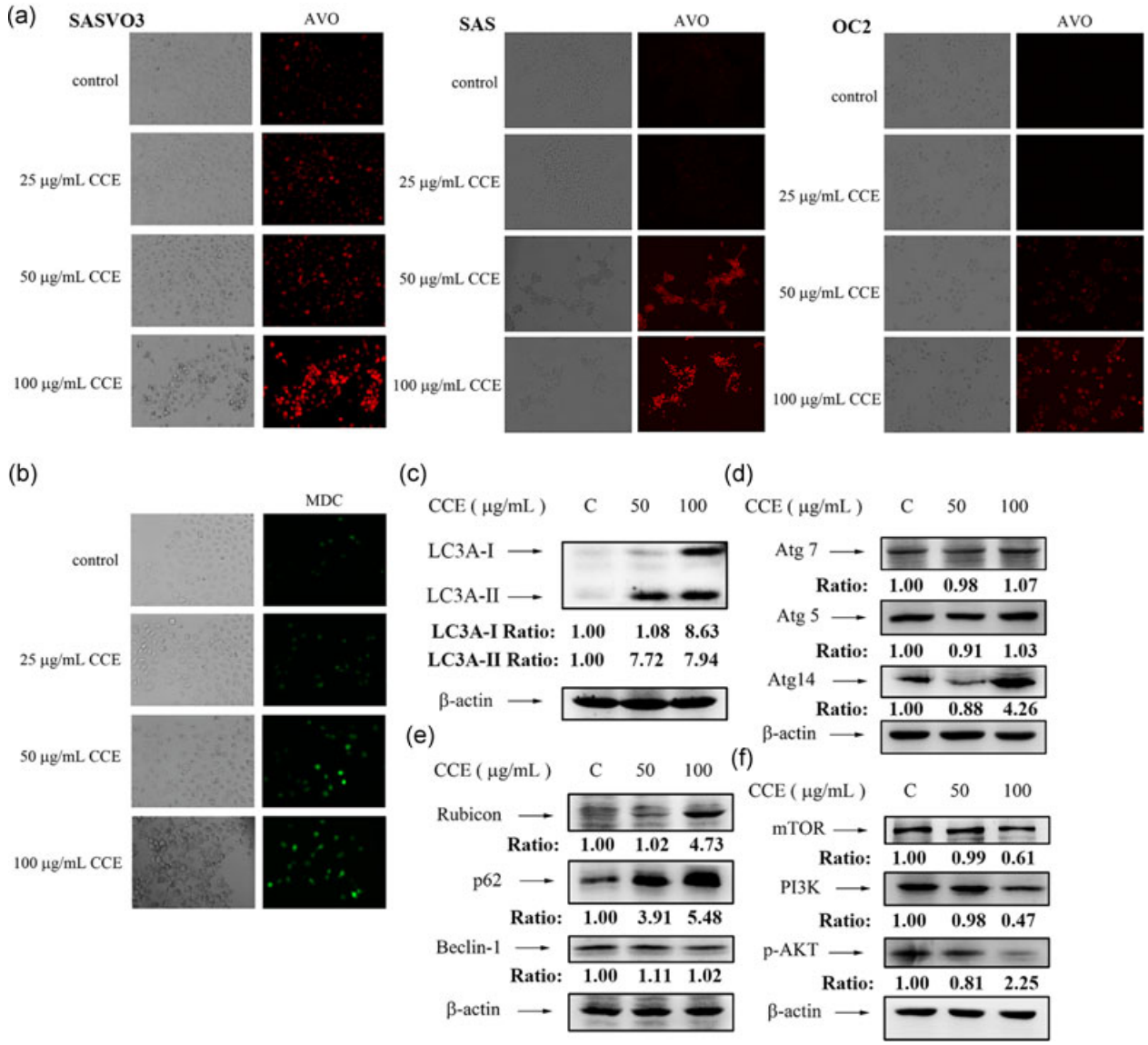

FIGURE 4 Induction of autophagy by CCE in SASVO3 cells. (a) AVO was detected using a fluorescence microscope. CCE induced the AVO formation in SASVO3, SAS, and OC2 cells. (b) After MDC staining was performed, the cells were visualized under a fluorescence microscope. CCE elevated the MDC-labeled autophagosomes in SASVO3 cells. Western blot analysis was conducted to evaluate (c) LC3-I, LC3-II, (d) Atg7, Atg8, Atg14, (e) rubicon, p62, Beclin-1, (f) mTOR, PI3K, and p-AKT. β-Actin was used as an internal control. The result representing the three separate experiments is shown. Atg: autophagy; AVO: acidic vesicular organelle; CCE: *Cinnamomum cassia* extract; LC3: light chain 3; MDC: monodansylcadaverine; mTOR: mammalian target of rapamycin; PI3K: phosphoinositide 3-kinase [Color figure can be viewed at wileyonlinelibrary.com]

The results showed that CCE increased the proportion of the cells in these three quadrants, especially in the upper right quadrant containing apoptotic or necrotic cells in SASVO3 and SAS cells. At 100 μg/ml, CCE elevated the percentage of annexin V/PI-positive cells to 23.7% and 9.2% in SASVO3 and SAS cells, respectively (Figure 2d).

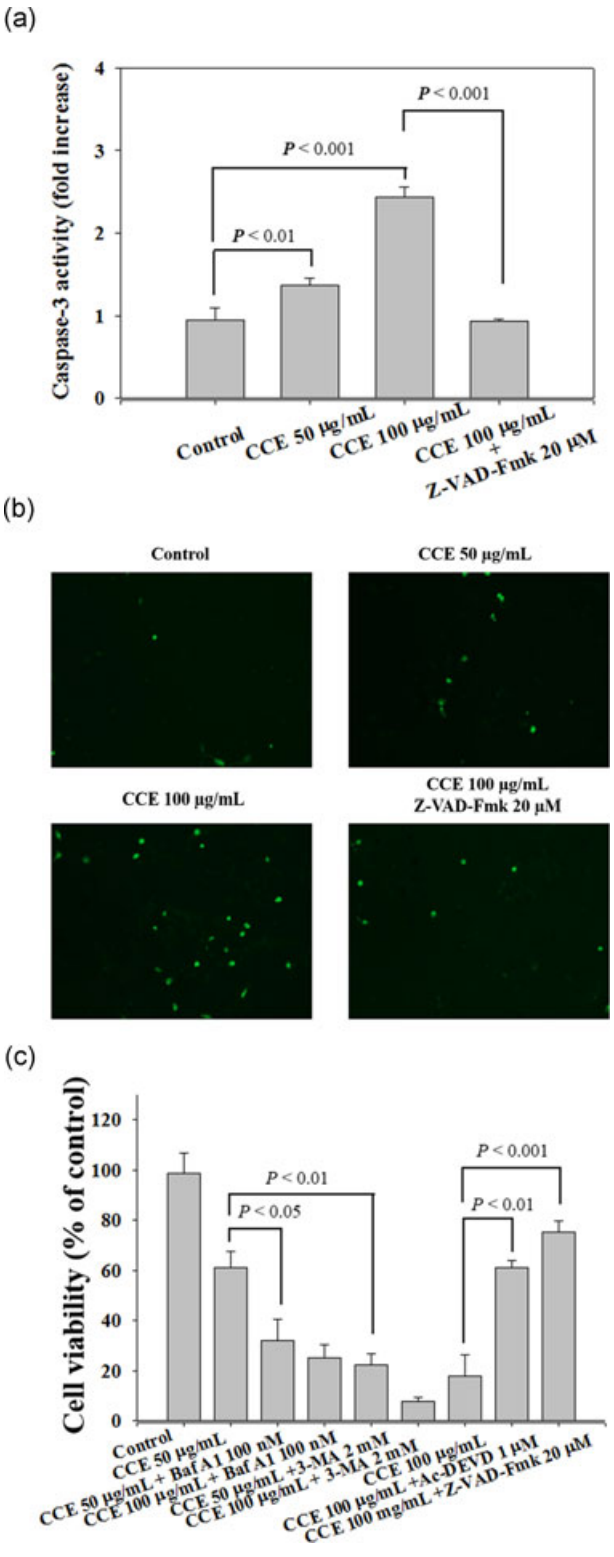

To examine whether CCE-induced apoptosis in SASVO3 cells, $\Delta\Psi_m$ and apoptotically nuclear morphology were, respectively, detected through JC-1 and DAPI staining after 24 hr of treatment. In Figure 3a, red fluorescence decreased and green fluorescence increased dose-dependently. This result indicated that CCE induced the membrane disruption of the mitochondria and then down-regulated $\Delta\Psi_m$. For the nuclear pattern, the chromatin condensed after CCE treatment (Figure 3b). In cell apoptosis, Bcl-2 family played an important role by promoting (e.g., Bax) or inhibiting (e.g., Bcl-2) the apoptotic mechanism. Subsequently, caspase-3 was activated to induce apoptotic cell death. Therefore, the activity kit and western blot were used to determine the expression of apoptotic molecules after the CCE treatment in both SASVO3 and SAS cells. CCE at 50–100 μg/ml significantly elevated the caspase-3 activity (Figure 3c), and this result could be confirmed by caspase-3 protein expression. In addition, antiapoptotic Bcl-2 was reduced after 24 hr of CCE treatment (Figure 3d). These results suggested CCE-induced apoptosis of both SASVO3 and SAS cells.

3.3 | CCE-induced autophagy of SASVO3 cells

Autophagy is one of the mechanisms that induce cancer cell death. In this study, acridine orange staining for AVO and MDC staining for autophagic vacuoles were performed to investigate whether autophagy participated in CCE-provoked cell death. The morphological characteristics of autophagy, AVO was enhanced in a dose-dependent manner as indicated by red in SASVO3, SAS, and OC2 cells (Figures 4a). Autophagic vacuoles were enhanced in a dose-dependent manner as indicated by green fluorescence in SASVO3 cells (Figures 4b). Western blot was then used to detect the protein expression of autophagy (Atg)-related molecules. Our previous studies suggested that Beclin-1, phosphoinositide 3-kinase (PI3K), rubicon, and autophagy-related family were effective in autophagy initiation and autophagosome formation (Chu, Hsieh, Yu, Lai, & Chen, 2014). In addition, microtubule-associated protein 1 light chain 3-I (LC3-I) directly binds to lipid phosphatidylethanolamine and then becomes implanted into the autophagic membrane to produce LC3-II, which is a marker for autophagy. By contrast, the mammalian target of rapamycin (mTOR) is a major negative regulator of autophagy. LC3A-I and LC3A-II dose-dependently increased after CCE treatment

FIGURE 5 CCE-induced activation of the apoptosis of SASVO3 cells. The cells were pretreated with or without Z-VAD-Fmk for 2 hr and then cultured with CCE for another 24 hr. (a) Caspase-3 activity was measured using an assay kit. (b) The cells were loaded with 5 μM CellEvent™ Caspase-3/7 Green Detection Reagent for 30 min. CCE-induced apoptosis was detected. The photos representing three separate experiments are shown. (c) The cells were pretreated with or without autophagy inhibitors (Baf A1 and 3-MA) or apoptosis inhibitors (Ac-DEVD-CHO and Z-VAD-Fmk) for 2 hr, and next treated with or without CCE for 24 hr. Cell viability was determined through an MTT assay. 3-MA: 3-methyladenine; Baf A1: bafilomycin A1; CCE: *Cinnamomum cassia* extract; MTT: 3-(4,5-dimethylthiazol-2-y1)-2,5-diphenyltetrazolium bromide [Color figure can be viewed at wileyonlinelibrary.com]

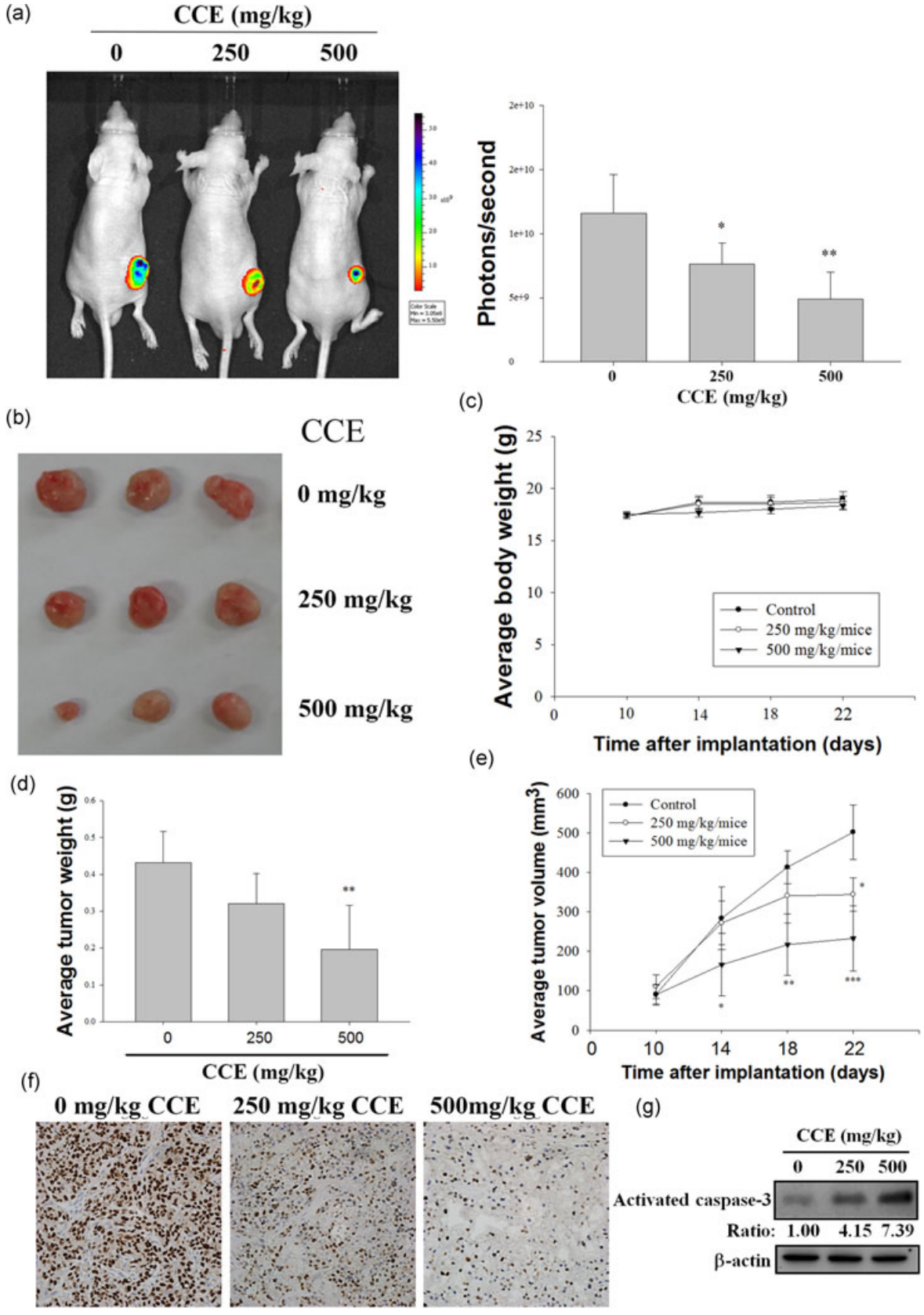

FIGURE 6 Continued.

was administrated in SASVO3 cells (Figure 4c). In the Atg family, only Atg14 was increased by 100 μg/ml CCE (Figure 4d). Rubicon and p62 were also stimulated after the CCE treatment was administrated, whereas Beclin-1 was not affected (Figure 4e). PI3K, Akt, and downstream mTOR were significantly inhibited by 100 μg/ml CCE (Figure 4f). Therefore, the mTOR pathway might be involved in CCE-induced autophagy.

3.4 | CCE-induced SASVO3 cell death via apoptosis rather than autophagy

Our results indicated that CCE induced both apoptosis and autophagy pathways. To further verify which one is the major pathway of CCE caused cell death, autophagy inhibitors (bafilomycin A1 [Baf A1] and 3-methyladenine [3-MA]) or apoptosis inhibitors (Ac-DEVD-CHO and Z-VAD-Fmk) were used. SASVO3 cells were pretreated with 20 μM Z-VAD-Fmk, a caspase inhibitor, for 2 hr and then treated with CCE for another 24 hr. CCE did increase caspase-3 activity, which was downregulated after the cells were preincubated with Z-VAD-Fmk ($p < 0.001$; Figure 5a). In addition, green fluorescence-labeled caspase-3/7 was also observed in a dose-dependent manner after the CCE treatment. In the presence of Z-VAD-Fmk, this observation was reduced (Figure 5b). In the cell viability assay, the pretreatment of caspase inhibitors (Ac-DEVD-CHO and Z-VAD-Fmk) significantly reversed the CCE-reduced viability ($p < 0.001$). However, the cotreatment of the autophagy inhibitors (Baf A1 and 3-MA) with CCE decreased the cell viability to a greater extent than the single CCE treatment ($p < 0.001$; Figure 5c). These data suggested that apoptosis induction was the major pathway of CCE-induced cell death, whereas CCE-induced autophagy was a survival mechanism of SASVO3 cells.

3.5 | Antitumorigenesis effects of CCE in vivo

Luciferase-expressing SASVO3 cells were subcutaneously inoculated into the right flank of the nude mice. After 10 days, the mice were fed with sterile water (control group) or various dosages of CCE to determine the in vivo antitumor effects of CCE. Fluorescence intensity is shown in Figure 6a. CCE remarkably inhibited the tumor growth after 12 days of feeding. This result was confirmed by the photo of representative tumors in each group and the average tumor weight, revealing 500 mg/kg CCE significantly reduced the tumor growth on Day 22 ($p < 0.01$; Figures 6b,d). The average tumor volumes were scaled down significantly by 500 mg/kg CCE treatment on days 14, 18 , and 22; and these values were 42%, 46%, and 55% lower than those of the control group, respectively. The low dosage of CCE (250 mg/kg) also reduced 32% of the tumor volume on Day 22 ($p < 0.05$). In addition, the body weight of the control and CCE groups did not differ throughout the experiment, suggesting that CCE did not cause any obvious toxic effects on the mice (Figure 6c). In the tumor of the control group, the proliferation marker Ki-67 was observed strongly. After 12 days of CCE treatment, the intensity of the Ki-67 stain decreased in a dose-dependent manner (Figure 6f). We assessed the expression of activated caspase-3 in the tumors collected from the control group (0 mg/kg) and CCE-fed mice (250 and 500 mg/kg) at the termination of the experiment. CCE showed a profound in vivo increased effect on activated caspase-3 expression by western blot analysis (Figure 6g).

3.6 | Bioactive components of CCE

To elucidate the major compounds of CCE becomes important for further investigations or clinical applications. A previous study found that coumarin, cinnamic acid, and cinnamic aldehyde are the bioactive components of *C. cassia*. In our study, three peaks were shown in the HPLC analysis (Figure 7a). Standard compounds were injected into HPLC, and the specific peaks of coumarin, cinnamic acid, and cinnamic aldehyde were found at 23.540, 25.193, and 27.589 min, respectively (Figure 7b–d). These peaks showed at the same time as those in Figure 7a. To further confirm that these three compounds were the components of CCE, the individual standard compounds were mixed with CCE and the HPLC analysis was performed. In Figure 7e–g, the standard compounds overlapped with the peak of CCE, suggesting that coumarin, cinnamic acid, and cinnamic aldehyde were the main constituents of *C. cassia*. SASVO3, SAS, and OC2 cells were treated with coumarin, cinnamic aldehyde, or cinnamic acid (0, 5, and 10 μM) for 24 hr and then cell viability was analyzed by MTT assay. Cinnamic aldehyde at 10 μM had significant inhibitory effects in SASVO3, SAS, and OC2 cells. However, coumarin and cinnamic acid did not affect these cells in the MTT assay (Figure 7h). To examine whether cinnamic aldehyde induced apoptosis in SASVO3 cells, apoptotically nuclear morphology was detected by DAPI staining after 24 hr of treatment. Chromatin condensation was observed in SASVO3 cells by DAPI staining (Figure 7i). Furthermore, the ability of cinnamic aldehyde to modulate the expression of caspase-3 and LC3A in SASVO3 cells were determined. Cinnamic aldehyde treatment resulted in a significant increase in the active subunit of caspase-3 (Figure 7j) and an increase in LC3A-II, a protein marker of autophagy, was observed after the cells

FIGURE 6 Antitumor effects of CCE in vivo. BALB/c nude mice ($N = 5$ for each group) were treated with either sterile water (placebo) or CCE after SASVO3 cells were subcutaneously (sc) implanted. Tumor growth was then detected. (a) BLI was performed 22 days after the treatment. (b) Representative tumors were isolated from mice 22 days after the initiation of the treatment. (c) Average body weight of the mice during the experiment. (d) The tumor weight of each mouse at the end of the treatment. (e) Tumor volume at each time interval during the treatment. (f) Ki-67 (cell proliferation marker) immunointensity in SASVO3 tumors. (g) Tumor tissues were homogenized and cell lysates were subjected to SDS-PAGE followed by western blot analysis. The membrane was probed with antiactivated caspase-3 antibody with β-actin as an internal control. $^{*}p < 0.05$, $^{**}p < 0.01$, and $^{***}p < 0.001$ compared with the control group (a, d) or findings on Day 10 (e). CCE: *Cinnamomum cassia* extract; BLI: bioluminescence imaging; SDS-PAGE: sodium dodecyl sulfate polyacrylamide gel electrophoresis [Color figure can be viewed at wileyonlinelibrary.com]

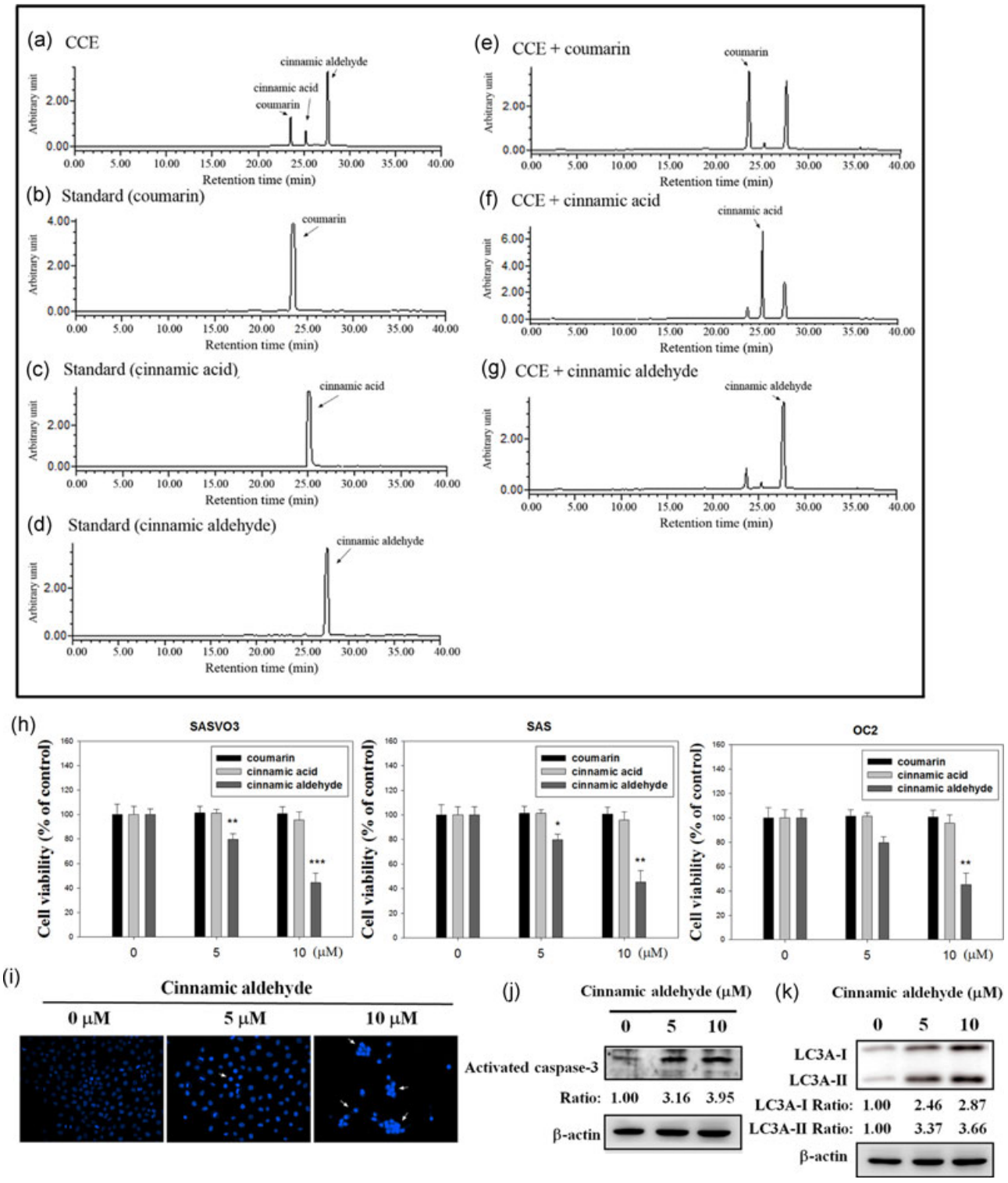

FIGURE 7 Chemical profiles of CCE analyzed through HPLC mass spectrometry and effects of cinnamic aldehyde in oral cancer cells. (a) Chromatographic patterns from the HPLC analysis of CCE showed peaks corresponding to the retention times (min). The peaks of the HPLC chromatogram indicated three kinds of the standard compound: (b) coumarin; (c) cinnamic acid; and (d) cinnamic aldehyde. (e) Combination of 200 μg of CCE with 5 μg of coumarin. (f) Combination of 200 μg of CCE with 40 μg of cinnamic acid. (g) Combination of 200 μg of CCE with 10 μg of cinnamic aldehyde. Absorbance was monitored at 280 nm. (h) SAS, SASVO3, and OC2 cells were treated with coumarin, cinnamic aldehyde, or cinnamic acid for 24 hr. Cell viability was analyzed by MTT assay. (i) SASVO3 cells were stained with DAPI, and treatment of cinnamic aldehyde showed the areas with intense fluorescence staining and condensed nuclei (at a magnification of ×100). In western blot assay, the membranes were probed with antibodies against activated caspase-3 (j), LC3A-I and LC3A-II (k), with β-actin being an internal control. CCE: *Cinnamomum cassia* extract; DAPI 4′,6-diamidino-2-phenylindole; HPLC: high-performance liquid chromatography; MTT: 3-(4,5-dimethylthiazol-2-y1)-2,5-diphenyltetrazolium bromide [Color figure can be viewed at wileyonlinelibrary.com]

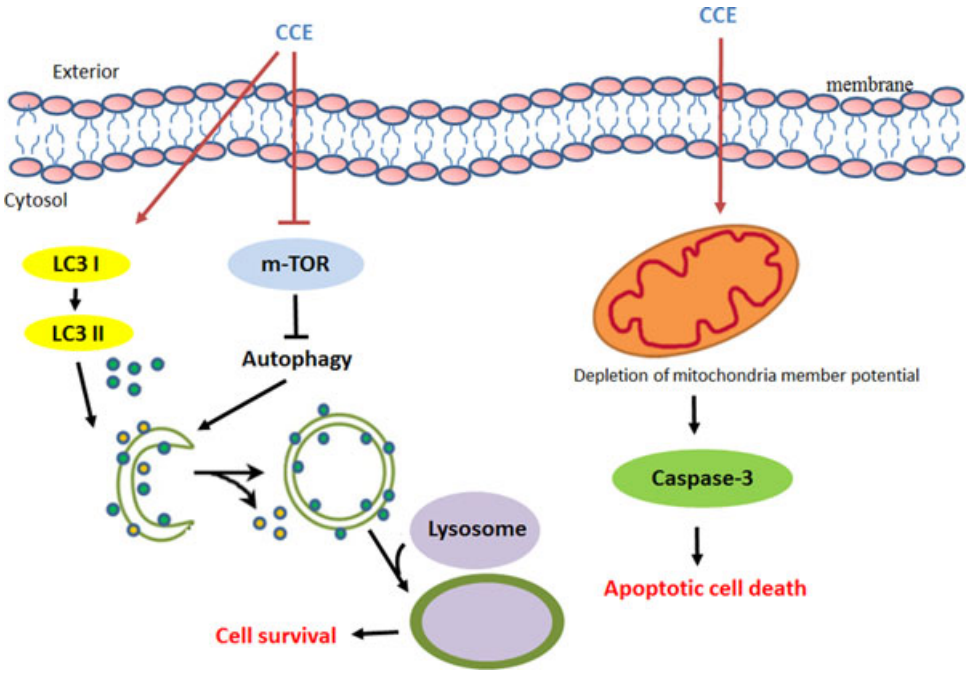

FIGURE 8 Proposed molecular targets of CCE with anticancer efficacy for SASVO3 cells. CCE induced the death of SASVO3 cells via apoptosis. Chromosome condensation, $\Delta\Psi_m$ collapse, and caspase-3 activation-dependent apoptosis were detected after CCE treatment. CCE-stimulated autophagy was a cell survival signaling, not a cell-death mechanism. CCE: *Cinnamomum cassia* extract [Color figure can be viewed at wileyonlinelibrary.com]

were treated with cinnamic aldehyde (Figure 7k). Altogether, cinnamic aldehyde seemed to possess the most potency of SASVO3 cellular effect among three bioactive compounds of CCE.

In summary, CCE caused the death of oral SASVO3 cancer cells in vitro and in vivo by inducing caspase-dependent apoptosis. The LC3-II-dependent autophagy pathway induced by CCE was the survival response of SASVO3 cells (Figure 8).

4 | DISCUSSION

Herbal compositions from natural products have been broadly investigated in the prevention and inhibition of cancer progression in early stages (Mohammadzadeh, Faramarzi, Mahdavi, Nasirimotlagh, & Asghari Jafarabadi, 2013). Although chemotherapy and target treatment have been applied to patients with cancer, adverse effects and drug resistance limit therapeutic procedures. To overcome these problems, researchers combined herbal compositions with clinical anticancer drugs, such as baicalein in thyroid cancer (C. H. Park, Han, Nam-Goong, Kim, & Kim, 2018), capiliposide C in esophageal cancer (Shen, Xu, Li, & Zhang, 2017), and astragalus polysaccharides in nasopharyngeal carcinoma (Zhou, Meng, & Ni, 2017). In our study, CCE could reduce human oral cancer cell growth in vitro and in vivo through apoptotic but not autophagic cell death.

Extensive studies have indicated that apoptosis is involved in the mechanism of cancer therapy. The cell membrane blebbing and permeability increase, DNA fragmentation, $\Delta\Psi_m$ decrease, phosphatidylserine inversion, and caspase-3 activation can be found in apoptotic cells (Kianpour Rad et al., 2015). ROS and its downstream NF-κB and ATF3 activation are involved in CCE-induced mitochondria-dependent apoptosis (S. H. Park, Song, et al., 2018). In this study, CCE significantly stimulated these apoptotic phenomena, including an increase in sub-G1 percentage, annexin V staining, caspase-3 activity, and a decrease of $\Delta\Psi_m$ and Bcl-2 expression (Figures 1-3). Elevation of ROS level might also be the trigger of subsequent mitochondria-dependent apoptosis in CCE-treated oral cancer cells.

However, the role of autophagy is ambiguous. It can be stimulated by starvation, cell survival, aging, and cell death. For the function involved in cell survival, autophagy is protective signaling for cancer cells under treatment. For the activity resulting in cell death, autophagy sensitizes the function of cancer therapy drugs. The factors that determine prosurvival or prodeath autophagic pathway remain unclear, but cell types and stress levels are certainly involved (Chu et al., 2014). During autophagy, autophagosomes form and fuse with lysosomes in the cytoplasm to degrade and recycle damaged organelles. Some proteins, such as LC3-I, Atg, and Becline-1 are expressed to facilitate this process (S. H. Kim et al., 2017). In our study, acridine orange-stained AVOs and MDC-stained autophagosomes strongly increased after CCE treatment (Figure 4). The inhibition of caspase activity significantly restored the cell viability, but the inhibition of autophagosome generation by 3-MA or the prevention of autolysosome formation by Baf A1 strengthened the effects of CCE (Figure 5). Therefore, CCE-induced autophagy in SASVO3 cells was a cell survival signaling but not a cell-death mechanism.

Crosstalks exist between apoptosis and autophagy. Some studies have revealed that autophagy is a protective mechanism against apoptosis (S. H. Kim et al., 2017), whereas other studies indicated

that strong autophagic signaling eventually led to autophagic cell death (S. H. Park et al., 2012). The apoptosis and autophagy of prostate cancer cells are stimulated by ROS triggered by deoxypodophyllotoixin (DPT), a natural phenol extracted from *Anthriscus sylvestris*. However, DPT-activated apoptosis is intensified by LC3 knockdown (S. H. Kim et al., 2017). Similar results are induced by sodium selenite through the generation of ROS and the stimulation of both apoptosis and autophagy in human lung cancer cells. The pretreatment of Baf A1 upregulates sodium selenite caused by apoptosis of cancer cells (S. H. Park et al., 2012). Accordingly, autophagy induced by DPT and sodium selenite functions as a protective mechanism against both treatments. These findings are consistent with the effects of CCE on human oral cancer cells.

CCE significantly reduced the SASVO3 oral tumor growth without affecting the body weight of the mice (Figure 6). To our knowledge, the current study is the first to illustrate the antitumor effects of CCE on oral cancer. Pharmacologists have designed a method to predict pharmacokinetic measures across species according to size and time (Boxenbaum & DiLea, 1995; Ings, 1990), and the conversion factor (km) is body weight per surface area. Therefore, the dose used in Species 1 is equal to ($km_{Species\ 2}/km_{Species\ 1}$) the time of the dose in Species 2. In our study, CCE doses of 250 and 500 mg/kg in mice might be comparable to 20.8 and 41.6 mg/kg in humans, respectively. These amounts of CCE might be applicable to clinical usage.

The major constituents of CCE used in this study were coumarin, cinnamic acid, and cinnamic aldehyde. These individual compounds possess anticancer activities in various cancers. For instance, cinnamic aldehyde elicits an antitumor effect on human colon cancer by suppressing β-catenin signaling (Lee, Park, Chung, Kim, & Lee, 2013). Cinnamic acid derivatives induce colon and cervical cancer cell death by inhibiting histone deacetylase (Anantharaju et al., 2017). Coumarin derivatives are potent inhibitor of many proteins, such as epidermal growth factor receptor, tyrosine kinase, and extracellular signal-regulated kinase 1/2 (ERK1/2). Therefore, coumarin has extensive anticancer activity in human lung cancer with minor adverse effects (Kumar, Singla, Dandriyal, & Jaitak, 2017). These findings indicated that CCE might also exhibit anticancer and antitumor effects on human oral cancer. In conclusion, CCE might show potential for the complementary treatment of patients with oral cancers. The inhibition of autophagy during CCE treatment should also be considered.

ACKNOWLEDGMENTS

This study was financially supported by clinical research grants from the Ministry of Science and Technology, Taiwan (MOST 106–2320-B-040-020-MY3 and MOST 106-2320-B-040-016).

CONFLICTS OF INTEREST

The authors declare that there are no conflicts of interest.

ORCID

Pei-Ni Chen http://orcid.org/0000-0002-4681-8719

REFERENCES

Anantharaju, P. G., Reddy, D. B., Padukudru, M. A., Chitturi, C. M. K., Vimalambike, M. G., & Madhunapantula, S. V. (2017). Induction of colon and cervical cancer cell death by cinnamic acid derivatives is mediated through the inhibition of histone deacetylases (HDAC). *PLOS One*, *12*, e0186208.

Boxenbaum, H., & DiLea, C. (1995). First-time-in-human dose selection: Allometric thoughts and perspectives. *Journal of Clinical Pharmacology*, *35*, 957–966.

Chang, W. L., Cheng, F. C., Wang, S. P., Chou, S. T., & Shih, Y. (2017). *Cinnamomum cassia* essential oil and its major constituent cinnamaldehyde induced cell cycle arrest and apoptosis in human oral squamous cell carcinoma HSC-3 cells. *Environmental Toxicology*, *32*, 456–468.

Chen, C. Y., Chiou, S. H., Huang, C. Y., Jan, C. I., Lin, S. C., Tsai, M. L., & Lo, J. F. (2009). Distinct population of highly malignant cells in a head and neck squamous cell carcinoma cell line established by xenograft model. *Journal of Biomedical Science*, *16*, 100.

Chen, P. N., Chu, S. C., Chiou, H. L., Chiang, C. L., Yang, S. F., & Hsieh, Y. S. (2005). Cyanidin 3-glucoside and peonidin 3-glucoside inhibit tumor cell growth and induce apoptosis in vitro and suppress tumor growth in vivo. *Nutrition and Cancer*, *53*, 232–243.

Chen, P. N., Chu, S. C., Kuo, W. H., Chou, M. Y., Lin, J. K., & Hsieh, Y. S. (2011). Epigallocatechin-3 gallate inhibits invasion, epithelial-mesenchymal transition, and tumor growth in oral cancer cells. *Journal of Agricultural and Food Chemistry*, *59*, 3836–3844.

Chen, P. N., Hsieh, Y. S., Chiang, C. L., Chiou, H. L., Yang, S. F., & Chu, S. C. (2006). Silibinin inhibits invasion of oral cancer cells by suppressing the mapk pathway. *Journal of Dental Research*, *85*, 220–225.

Chen, S. F., Chang, Y. C., Nieh, S., Liu, C. L., Yang, C. Y., & Lin, Y. S. (2012). Nonadhesive culture system as a model of rapid sphere formation with cancer stem cell properties. *PLOS One*, *7*, e31864.

Chu, S. C., Hsieh, Y. S., Yu, C. C., Lai, Y. Y., & Chen, P. N. (2014). Thymoquinone induces cell death in human squamous carcinoma cells via caspase activation-dependent apoptosis and LC3-II activation-dependent autophagy. *PLOS One*, *9*, e101579.

Fatima, M., Zaidi, N. S. S., Amraiz, D., & Afzal, F. (2016). In vitro antiviral activity of *Cinnamomum cassia* and its nanoparticles against H7N3 influenza a virus. *Journal of Microbiology and Biotechnology*, *26*, 151–159.

Goswami, S. K., Inamdar, M. N., Jamwal, R., & Dethe, S. (2014). Effect of *Cinnamomum cassia* methanol extract and sildenafil on arginase and sexual function of young male wistar rats. *The Journal of Sexual Medicine*, *11*, 1475–1483.

Ho, Y. S., Duh, J. S., Jeng, J. H., Wang, Y. J., Liang, Y. C., Lin, C. H., … Lin, J. K. (2001). Griseofulvin potentiates antitumorigenesis effects of nocodazole through induction of apoptosis and G2/M cell cycle arrest in human colorectal cancer cells. *International Journal of Cancer*, *91*, 393–401.

Hsieh, Y. S., Chu, S. C., Hsu, L. S., Chen, K. S., Lai, M. T., Yeh, C. H., & Chen, P. N. (2013). *Rubus idaeus* l. Reverses epithelial-to-mesenchymal transition and suppresses cell invasion and protease activities by targeting ERK1/2 and fak pathways in human lung cancer cells. *Food and Chemical Toxicology*, *62*, 908–918.

Hsin, I. L., Ou, C. C., Wu, T. C., Jan, M. S., Wu, M. F., Chiu, L. Y., … Ko, J. L. (2011). GMI, an immunomodulatory protein from ganoderma microsporum, induces autophagy in non-small cell lung cancer cells. *Autophagy*, *7*, 873–882.

Hu, F. W., Tsai, L. L., Yu, C. H., Chen, P. N., Chou, M. Y., & Yu, C. C. (2012). Impairment of tumor-initiating stem-like property and reversal of epithelial-mesenchymal transdifferentiation in head and neck cancer

by resveratrol treatment. *Molecular Nutrition & Food Research*, *56*, 1247–1258.

Huang, S. F., Horng, C. T., Hsieh, Y. S., Hsieh, Y. H., Chu, S. C., & Chen, P. N. (2016). Epicatechin-3-gallate reverses TGF-beta1-induced epithelial-to-mesenchymal transition and inhibits cell invasion and protease activities in human lung cancer cells. *Food and Chemical Toxicology*, *94*, 1–10.

Huh, J. E., Kim, S. J., Kang, J. W., Nam, D. W., Choi, D. Y., Park, D. S., & Lee, J. D. (2015). The standardized BHH10 extract, a combination of astragalus membranaceus, *Cinnamomum cassia*, and *Phellodendron amurense*, reverses bone mass and metabolism in a rat model of postmenopausal osteoporosis. *Phytotherapy Research*, *29*, 30–39.

Ings, R. M. J. (1990). Interspecies scaling and comparisons in drug development and toxicokinetics. *Xenobiotica*, *20*, 1201–1231.

Jacobson, J. J., Epstein, J. B., Eichmiller, F. C., Gibson, T. B., Carls, G. S., Vogtmann, E., … Murphy, B. (2012). The cost burden of oral, oral pharyngeal, and salivary gland cancers in three groups: Commercial insurance, medicare, and medicaid. *Head & Neck Oncology*, *4*, 15.

Kianpour Rad, S., Kanthimathi, M. S., Abd Malek, S. N., Lee, G. S., Looi, C. Y., & Wong, W. F. (2015). *Cinnamomum cassia* suppresses caspase-9 through stimulation of AKT1 in MCF-7 cells but not in MDA-MB-231 cells. *PLOS One*, *10*, e0145216.

Kim, E. C., Kim, H. J., & Kim, T. J. (2015). Water extract of *Cinnamomum cassia* suppresses angiogenesis through inhibition of VEGF receptor 2 phosphorylation. *Bioscience, Biotechnology, and Biochemistry*, *79*, 617–624.

Kim, S. H., Kim, K. Y., Park, S. G., Yu, S. N., Kim, Y. W., Nam, H. W., … Ahn, S. C. (2017). Mitochondrial ROS activates ERK/autophagy pathway as a protected mechanism against deoxypodophyllotoxin-induced apoptosis. *Oncotarget*, *8*, 111581–111596.

Kumar, M., Singla, R., Dandriyal, J., & Jaitak, V. (2017). Coumarin derivatives as anticancer agents for lung cancer therapy: A review. *Anti-cancer Agents in Medicinal Chemistry*, *18*

Lee, M. A., Park, H. J., Chung, H. J., Kim, W. K., & Lee, S. K. (2013). Antitumor activity of 2-hydroxycinnamaldehyde for human colon cancer cells through suppression of beta-catenin signaling. *Journal of Natural Products*, *76*, 1278–1284.

Liao, J. C., Deng, J. S., Chiu, C. S., Hou, W. C., Huang, S. S., Shie, P. H., & Huang, G. J. (2012). Anti-inflammatory activities of *Cinnamomum cassia* constituents in vitro and in vivo. *Evidence-Based Complementary and Alternative Medicine*, *2012*, 429320.

Lin, C. Y., Hsieh, Y. H., Yang, S. F., Chu, S. C., Chen, P. N., & Hsieh, Y. S. (2017). *Cinnamomum cassia* extracts reverses TGF-beta1-induced epithelial-mesenchymal transition in human lung adenocarcinoma cells and suppresses tumor growth in vivo. *Environmental Toxicology*, *32*, 1878–1887.

Lu, K. H., Chen, P. N., Hsieh, Y. H., Lin, C. Y., Cheng, F. Y., Chiu, P. C., … Hsieh, Y. S. (2016). 3-Hydroxyflavone inhibits human osteosarcoma U2OS and 143B cells metastasis by affecting EMT and repressing u-PA/MMP-2 via FAK-Src to MEK/ERK and RhoA/MLC2 pathways and reduces 143B tumor growth in vivo. *Food and Chemical Toxicology*, *97*, 177–186.

Mantena, S. K., Sharma, S. D., & Katiyar, S. K. (2006). Berberine, a natural product, induces G1-phase cell cycle arrest and caspase-3-dependent apoptosis in human prostate carcinoma cells. *Molecular Cancer Therapeutics*, *5*, 296–308.

Mohammadzadeh, M., Faramarzi, E., Mahdavi, R., Nasirimotlagh, B., & Asghari Jafarabadi, M. (2013). Effect of conjugated linoleic acid supplementation on inflammatory factors and matrix metalloproteinase enzymes in rectal cancer patients undergoing chemoradiotherapy. *Integrative Cancer Therapies*, *12*, 496–502.

Park, C. H., Han, S. E., Nam-Goong, I. S., Kim, Y. I., & Kim, E. S. (2018). Combined effects of baicalein and docetaxel on apoptosis in 8505c anaplastic thyroid cancer cells via downregulation of the ERK and akt/mtor pathways. *Endocrinology and Metabolism*, *33*, 121–132.

Park, G. H., Song, H. M., Park, S. B., Son, H. J., Um, Y., Kim, H. S., & Jeong, J. B. (2018). Cytotoxic activity of the twigs of *Cinnamomum cassia* through the suppression of cell proliferation and the induction of apoptosis in human colorectal cancer cells. *BMC Complementary and Alternative Medicine*, *18*, 28.

Park, S. H., Kim, J. H., Chi, G. Y., Kim, G. Y., Chang, Y. C., Moon, S. K., … Choi, Y. H. (2012). Induction of apoptosis and autophagy by sodium selenite in a549 human lung carcinoma cells through generation of reactive oxygen species. *Toxicology Letters*, *212*, 252–261.

Ranasinghe, P., Galappaththy, P., Constantine, G. R., Jayawardena, R., Weeratunga, H. D., Premakumara, S., & Katulanda, P. (2017). *Cinnamomum zeylanicum* (*Ceylon cinnamon*) as a potential pharmaceutical agent for type-2 diabetes mellitus: Study protocol for a randomized controlled trial. *Trials*, *18*, 446.

Shen, Z., Xu, L., Li, J., & Zhang, N. (2017). Capilliposide c sensitizes esophageal squamous carcinoma cells to oxaliplatin by inducing apoptosis through the PI3K/AKT/mTOR pathway. *Medical Science Monitor*, *23*, 2096–2103.

Shin, W. Y., Shim, D. W., Kim, M. K., Sun, X., Koppula, S., Yu, S. H., … Lee, K. H. (2017). Protective effects of *Cinnamomum cassia* (lamaceae) against gout and septic responses via attenuation of inflammasome activation in experimental models. *Journal of Ethnopharmacology*, *205*, 173–177.

Siegel, R. L., Miller, K. D., & Jemal, A. (2018). Cancer statistics, 2018. *CA: A Cancer Journal for Clinicians*, *68*, 7–30.

Song, M. Y., Kang, S. Y., Kang, A., Hwang, J. H., Park, Y. K., & Jung, H. W. (2017). *Cinnamomum cassia* prevents high-fat diet-induced obesity in mice through the increase of muscle energy. *American Journal of Chinese Medicine*, *45*, 1017–1031.

Tian, F., Yu, C. T., Ye, W. D., & Wang, Q. (2017). Cinnamaldehyde induces cell apoptosis mediated by a novel circular RNA hsa_circ_0043256 in non-small cell lung cancer. *Biochemical and Biophysical Research Communications*, *493*, 1260–1266.

Wong, D. Y. K., Chang, K. W., Chen, C. F., & Chang, R. C. S. (1990). Characterization of two new cell lines derived from oral cavity human squamous cell carcinomas—OC1 and OC2. *Journal of Oral and Maxillofacial Surgery*, *48*, 385–390.

Wu, C., Zhuang, Y., Jiang, S., Tian, F., Teng, Y., Chen, X., … Zou, X. (2017). Cinnamaldehyde induces apoptosis and reverses epithelial-mesenchymal transition through inhibition of Wnt/beta-catenin pathway in non-small cell lung cancer. *International Journal of Biochemistry and Cell Biology*, *84*, 58–74.

Wu, H. C., Horng, C. T., Lee, Y. L., Chen, P. N., Lin, C. Y., Liao, C. Y., … Chu, S. C. (2018). *Cinnamomum cassia* extracts suppress human lung cancer cells invasion by reducing u-PA/MMP expression through the FAK to ERK pathways. *International Journal of Medical Sciences*, *15*, 115–123.

Zada, W., Zeeshan, S., Bhatti, H. A., Mahmood, W., Rauf, K., & Abbas, G. (2016). *Cinnamomum cassia*: An implication of serotonin reuptake inhibition in animal models of depression. *Natural Product Research*, *30*, 1212–1214.

Zhou, Z., Meng, M., & Ni, H. (2017). Chemosensitizing effect of astragalus polysaccharides on nasopharyngeal carcinoma cells by inducing apoptosis and modulating expression of Bax/Bcl-2 ratio and caspases. *Medical Science Monitor*, *23*, 462–469.

How to cite this article: Yu C-H, Chu S-C, Yang S-F, Hsieh Y-S, Lee C-Y, Chen P-N. Induction of apoptotic but not autophagic cell death by *Cinnamomum cassia* extracts on human oral cancer cells. *J Cell Physiol*. 2019;234:5289–5303.
https://doi.org/10.1002/jcp.27338